Journal of Fluorescence (2018) 28:759–765
https://doi.org/10.1007/s10895-018-2237-0

ORIGINAL ARTICLE

Highly Sensitive and Selective Detection of Amoxicillin Using Carbon Quantum Dots Derived from Beet

Kunjie Wang[1] · Qingjuan Ji[1] · Jialin Xu[1] · Hongxia Li[1] · Deyi Zhang[1] · Xiaoyu Liu[1] · Yujuan Wu[1] · Haiyan Fan[2]

Received: 17 February 2018 / Accepted: 11 May 2018 / Published online: 19 May 2018

Abstract
In the present work, we synthesized the carbon quantum dots (CQDs) by one step hydrothermal method using the dried beet powder as the carbon source without additional chemical reagents and functionalization. The as-prepared CQDs are quasi-spherical carbon nanoparticles with diameters of 4–8 nm as well as surface functional groups such as carboxyl and hydroxyl groups, and exhibit good water-solubility, biocompatibility, and strong fluorescence. It is confirmed that amoxicillin (AMO) could enhance the fluorescent intensity of CQDs, the I/I_0 showed a linear correlation between the intensity of fluorescence and the concentration of AMO in a broad range. These superior properties render a potential application of the CQDs in biomedical.

Keywords Carbon quantum dots · Detection · Amoxicillin · Fluorescent enhanced

Introduction

Amoxicillin (AMO), semi-synthetic penicillins broad-spectrum β-lactam antibiotics, has been commonly used to treat the bacterial infections caused by gram-negative and gram-positive organisms, exogenous febrile disease and other common bacterial infections of humans as well as of agricultural livestock [1–3]. The chemical structures of AMO is shown in Fig. 1. Although it is very efficient, excessive use of AMO is quite harmful to human body, animals, and the environment, such as the allergy, toxicity, double infection. Especially, the excessive use of antibiotics in ambulatory practice has leaded to the emergence and spread of antibiotic-resistant bacteria [4, 5]. Hence, the development of an effective analytical approaches for sensitive and selective detection of trace amounts of AMO becomes essential. So far, several methods such as high-performance liquid chromatography (HPLC) [6], low injection chemi-luminescence [7], spectrophotometric [3], mass spectrometry [8], atomic absorption spectrophotometry [9], electrochemical techniques [10] have been applied to the quantification of AMO. However, most of the methods suffer from some limitations including low sensitivity, high cost, complicated operating process, and not hospital friendliness of some instruments. Therefore, it is urgent to develop a simple, effective, convenient, economical, and eco-environment detective strategy to quantitatively detect the amount of AMO in blood sample.

The carbon quantum dots (CQDs) [11], once discovered, have been intensively studied in the areas of catalysis [12, 13], bioimaging [14], medical diagnosis [15], and sensor [16, 17]. In particular, CQDs have been used as the biosensor to detect some cations, anions and organics such as Fe^{3+} [18–20], Cr^{5+} [21], Mo^{6+} [22], Co^{2+} [23], Hg^{2+} [24, 25], I^- [26], $ONOO^-$ [27], testosterone [28], hyaluronidase [29], selenite [30], glutathione [31] and tetracycline [32], taking advantage of its strong photoluminescence (PL), easy synthesis, excellent water solubility, biocompatibility, low toxicity, photobleachin resistance and environmental-friendliness [33–35].

Beet, on the other hand, is readily available, inexpensive, rich in sucrose and other carbohydrates, and mainly used for producing granulated sugar, which is suitable for be precursor of CQDs. Herein, we report the novel strategy to prepare the CQDs utilized the beet as the carbon source without adding additional agents for hydrothermal preparation. In addition, AMO can effectively enhance the PL intensity of as-prepared CQDs, and the I/I_0 and concentration of AMO has a certain linear reaction in a broad range.

✉ Kunjie Wang
Wangkj80@163.com

[1] College of Petrochemical Technology, Lanzhou University of Technology, Lanzhou 730050, China

[2] Chemistry Department, Nazarbayev University, Astana, Kazakhstan 010000

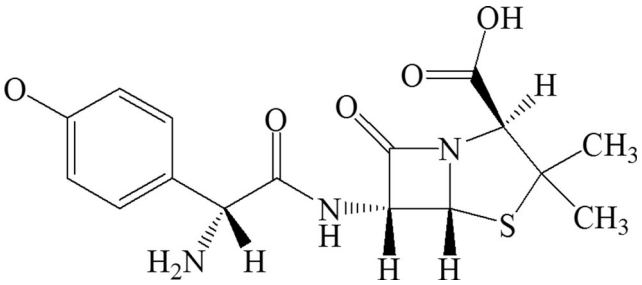

Fig. 1 The chemical structures of AMO

Experimental

Materials

Beet was purchased from the local market in Astana, Kazakhstan. Amoxicillin(98%) were obtained from Shanghai Yuanye Biological Technology Co., Ltd.. Phosphate-buffered saline(PBS) (PH = 6.8) were purchased from Shanghai Hongbei Reagent Co., Ltd.. Sucrose, glucose, ascorbic acid, tryptophan, aspartic acid, L-cysteine, KBr, $Ca(NO_3)_2$, NaF. All regents used were analytically pure (AR) and as received without further purification. Deionized water was prepared with a Milli-Q-Plus system(18.2 MΩ).

Characterization

Transmission electron microscopy (TEM) analyses were carried out using a JEOL JEM2100 instrument operating at 200 kV. The samples for TEM analysis were prepared by dropping a droplet of the ethanol solution of the product onto carbon-coated copper grids and drying at room temperature. Fourier transform infrared spectroscopy (FTIR) spectra were measured on a Nicolet AVATAR 360 FT-IR spectrophotometer. X-ray diffraction (XRD) analysis was carried out using a Shimadzu XRD-6000 spectrometer. PL and UV-vis spectra of the as-prepared CQDs were taken at room temperature in water. The PL spectra was performed with a LS-55 spectrophotometer (PerkinElmer, USA) and UV-vis spectra were obtained using a UV-2102PC spectrophotometer (Unico, USA). All optical measurements were carried out at room temperature under ambient conditions.

Synthesize of CQDs

The CQDs were prepared using the hydrothermal method, which we have reported previously [36]. Briefly, 1 g of the dried beetroot powder was added into 50 mL water. Then the mixture was transferred into a 100 mL Teflon-lined autoclave and heated at 200 °C in air dry oven for a period of 5 h. The crude product was obtained by filtration through a 0.22 μm millipore membrane and then dried in the oven at 60 °C. Thereafter, the crude product was re-dissolved in ethanol, filtrated by 0.22 μm millipore membrane. Finally, the CQDs was obtained by evaporating ethanol and further dried under vacuum oven. The as-prepared CQDs stored at 4 °C before use.

AMO Detection Using CQDs

To demonstrate sensing capability of the as-prepared CQDs, the sensing study was done with PL spectroscopy using different concentrations of AMO (0–400 μM). To affirm the stability of CQDs under high ionic strength conditions, their PL intensities were measured under high ionic strength conditions. To verify the selectivity, some common ions and small molecules were studied. All the PL intensity detections were carried out with an excitation wavelength at 380 nm (CQDs, 5 $\mu g \cdot mL^{-1}$). All the measurements were performed under the same conditions at room temperature, and repeated at least 3 times.

Results and Discussion

The Synthesis and Characterization of CQDs

Figure 2a displays the TEM patterns of the as-prepared CQDs. These CQDs are well dispersed and display uniform diameters in the range of 4–8 nm. Figure 1b shows the XRD spectrum of the as-prepared CQDs. The diffraction peak is at 23° is observed, suggesting that the CQDs are formed by highly disordered carbon atoms. Fourier transform infrared (FTIR) measurement was used to confirm the as-prepared CQDs and investigate the functional group in surface of these CQDs. As shown in Fig. 2c, the broad peak centered at 3419 cm^{-1} represents O-H bonding, and the absorption at 2929 cm^{-1} is attributed to C-H stretching vibrations. Two bands located at 1588 and 1384 cm^{-1} can only be assigned as the asymmetric and symmetric stretching vibrations of the carboxyl anions, respectively. It turns out the O-H group identified through the band at 3419 cm^{-1} is not necessarily the hydroxyl in carboxylic acids and the O-H group and carboxyl anions stay independently on the surface of CQDs. Therefore, the CQD prepared in the present work shows high water solubility.

The surface composition of the as-prepared CQDs were further confirmed by XPS. The full range XPS analysis (Fig. 3a) showed three peaks at 285.08, 401.08, and 533.08 eV corresponding to C1s, N1 s, and O1s, respectively. Figure 3b displayed the C1s spectrum which exist three peaks at 284.7, 285.7 and 286.8 eV, representing C1s states in C-C/C-H/C-O, C-N and C=O functionalities, respectively. The XPS spectrum of O1s exhibited three apparent peaks centered at 532.0 eV, 532.6 eV and 532.7 eV, which were related to the -OH, O-C/C-OH/O-C-O and C=O bond (Fig. 3c.). The high-resolution spectrum of N1 s can be assigned to two surface components in the as-prepared CQDs, corresponding to N-H at binding energy of 400.2 eV, as well as C-N at 402.4 eV (Fig.

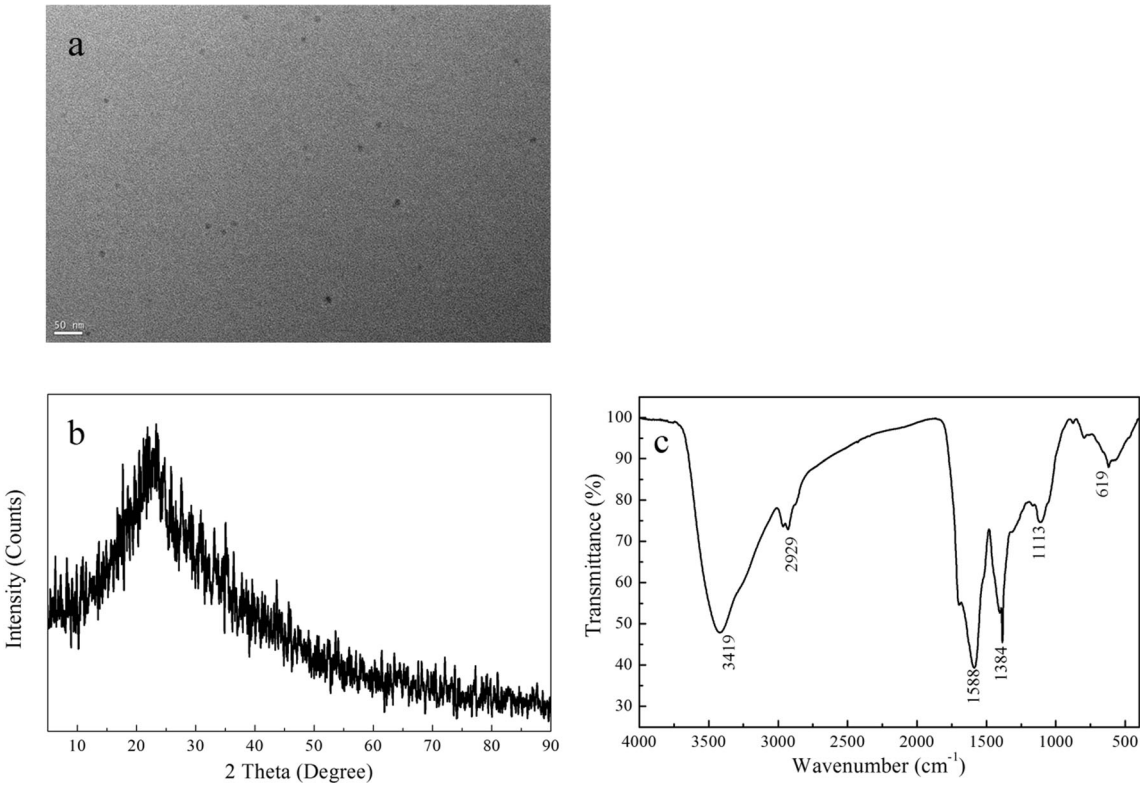

Fig. 2 TEM image (**a**); XRD pattern (**b**); and (**c**) FTIR spectra of the as-prepared CQDs

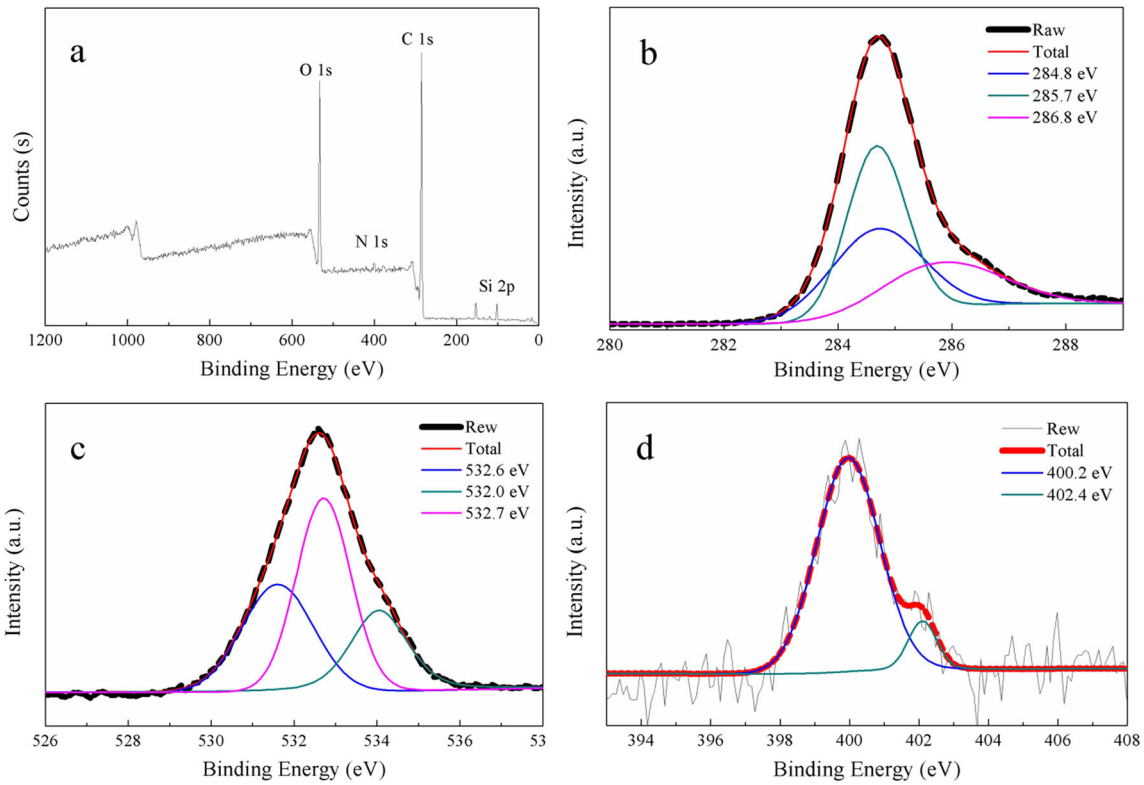

Fig. 3 XPS survey scan of (**a**) as-prepared CQDs; **b** High-resolution of C1s peaks; **c** High-resolution of O1s peaks and (**d**) High-resolution of N1 s peaks

3d). Although lacking the evidence from FTIR, the XPS results indicate there is certain nitrogen containing in beet, which makes beet a great starting material for the synthesis of CQDs. On the other hand, the existence of hydroxyl and carboxylic groups on the surface of as-prepared CQDs is supported by XPS test.

The UV-vis absorption spectrum shows three bands at 219 nm, 265 nm, and 330 nm as in Fig. 4a. While the band at 219 nm is corresponding to the π-π* transition of C=C, the absorptions at 265 nm and 330 nm represent n-π* transition of C=O bonds.

In order to further explore their PL properties, the PL variation of CQDs with different excited wavelength was investigated. Aqueous solution of the as-prepared CQDs exhibits excitation-dependent emission, as shown in Fig. 4b, the emission peaks are red shifted from 438 nm to 456 nm for the as-prepared CQDs as the excited wavelength moves from 340 to 400 nm. Moreover, the intensity of the emission peaks becomes strong and then weak with the increasing excited wavelength. This intrinsic property is duo to the different particle sizes and considerable distribution of emissive trap sites on the as-prepared CQDs, which has been reported previously [37].

Although the mechanism of the PL of CQDs remains unrevealed, the PL is known highly correlated to the states, distribution, and their association of the functional groups on the surface [38]. The effect of pH on the PL intensity of the as-prepared CQDs were studied under various pH solutions (1.0 to 14.0) (HCl and NaOH was used to adjust the pH of the system). A slight pH dependence was revealed and the optimized PL intensity of CQDs was achieved at pH = 6 (Fig. 5a).

The dependence of ionic strength of the fluorescent property of the as-prepared CQDs was estimated in the NaCl solution with the concentration from 0 to 1.0 M. As shown in Fig. 5b, interestingly, the PL intensity barely showed any dependence on the ionic strength. This is particularly an advantage for the measurement under high ionic strength conditions. This finding ensures that CQDs have great potential for sensing applications under more complicated conditions and physiological conditions.

Determination of AMO

Taking the advantages above, the as-prepared CQDs were utilized as a fluorescent sensor for sensitive and selective detection of AMO. Figure 6a depicted the change of PL intensity of the as-prepared CQDs in the presence of PBS and different concentration of AMO (0, 25, 50, 75, 100, 125, 150, 175, 200, 225, 250, 275, 300, 325, 350, 375, 400 μM). Clearly, the fluorescence was enhanced gradually with the increase in the concentration of AMO. Meanwhile, the I/I_0 showed a good linear response with the concentration of AMO in the range of 0–400 μM (Fig. 6b). The linear equation was $I/I_0 = 0.99618 + 0.01352[\mathrm{AMO}]$ ($R^2 = 0.99946$, I and I_0 were the PL intensity in the presence and absence of AMO, respectively.), which suggests that the detection of AMO is completely feasible using the as-prepared CQDs. The lower limit of measurement of AMO was identified as 0.475 μM in the present work.

Figure 6c displays the stability of the PL intensity of the CQDs solution added AMO. The PL intensity of CQDs at 380 nm was enhanced immediately when the AMO was added into the solution. The PL intensity of the solution remains stable during the 6 min after mixing. The result implies that the enhancement of AMO to the CQDs occurs in a short period of time and the resulting fluorescence is stable within a period of time when the detection can be well arranged. This promises a fast, convenient and stable sensing of AMO using the as-prepared CQDs. To evaluate the selectivity of the as-prepared CQDs, some potential interfering compounds, including sucrose, glucose, ascorbic acid, tryptophan, aspartic acid, L-cysteine, KBr, $Ca(NO_3)_2$, NaF (250 μM for each) were investigated under the same conditions. As shown in Fig. 6d, the potential interferes caused minor signal fluctuations, while the PL intensity change caused by AMO could be clearly distinguished. Hence, the detection of AMO using as-prepared CQDs is highly selective. High sensitivity, fast response, high stability, large ionic strength duration, along with high selectivity makes the sensing system established in the present work fairly remarkable.

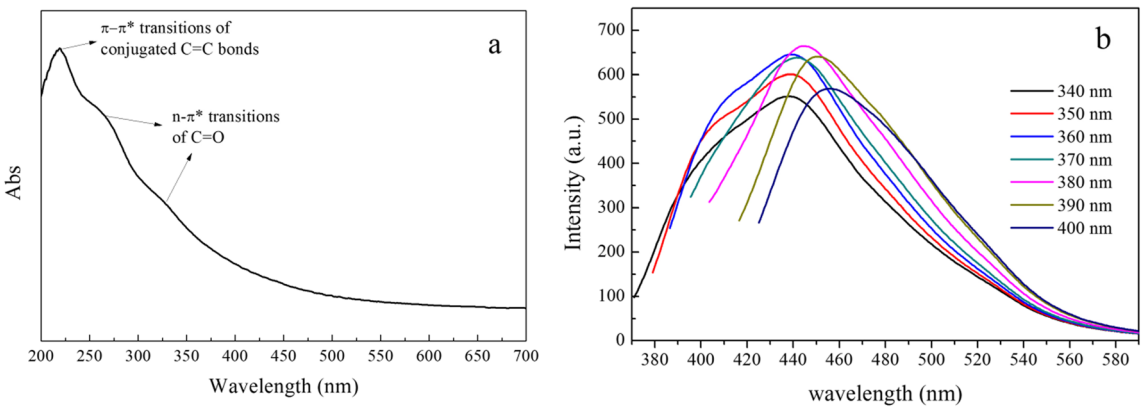

Fig. 4 **a** The UV-vis absorption spectrum of the as-prepared CQDs, and (**b**) the PL spectra of the as-prepared CQDs under a series of excited wavelength

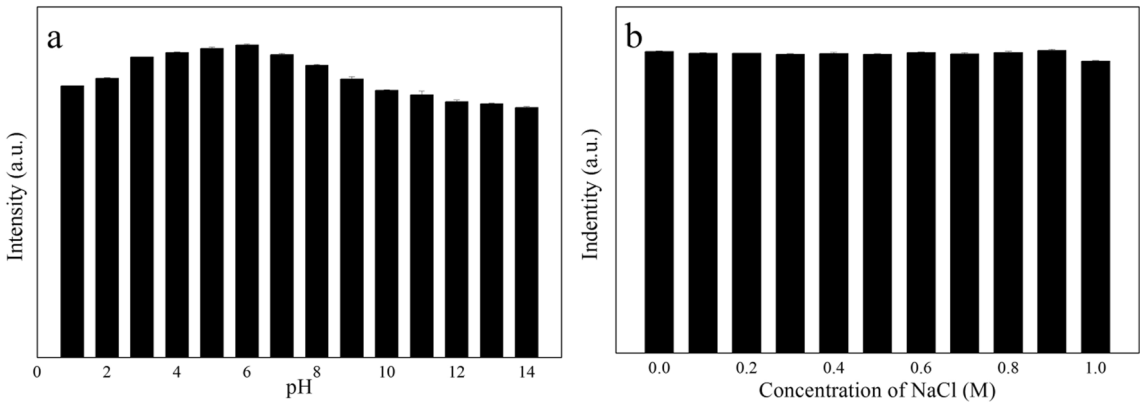

Fig. 5 **a** Effect of pH on the PL intensity of the as-prepared CQDs; **b** PL intensity of as-prepared CQDs in NaCl aqueous solution (pH = 7) against the ionic strength

The possible mechanism for the enhancement of the fluorescence will be further discussed below. Both FTIR and XPS indicate abundant hydrophilic groups (carboxylic and hydroxyl groups) are distributed on the surface of the as-prepared CQDs. While these functional groups promote the water solubility of CQDs, they also provide many potentials for the hydrogen bonding with AMO. Even though we do not know how exactly the hydrogen bonding with AMO changes or at least intervenes the electronic structure of the surface of CQDs, the binding with AMO in the present work certainly enhances the PL intensity [39]. On the other hand, the electrostatic repulsion between the AMO adsorbed on the surface of the CQDs would increase the distance between the CQDs, which would effectively separate the CQDs from each other, and further reduces the nonradiative decay. In addition, the attachment of AMO could potentially vary the surface defects of the CQDs, leading to the enhancement of PL intensity [40]. Nevertheless, the exact mechanism of enhancing fluorescence requires further study.

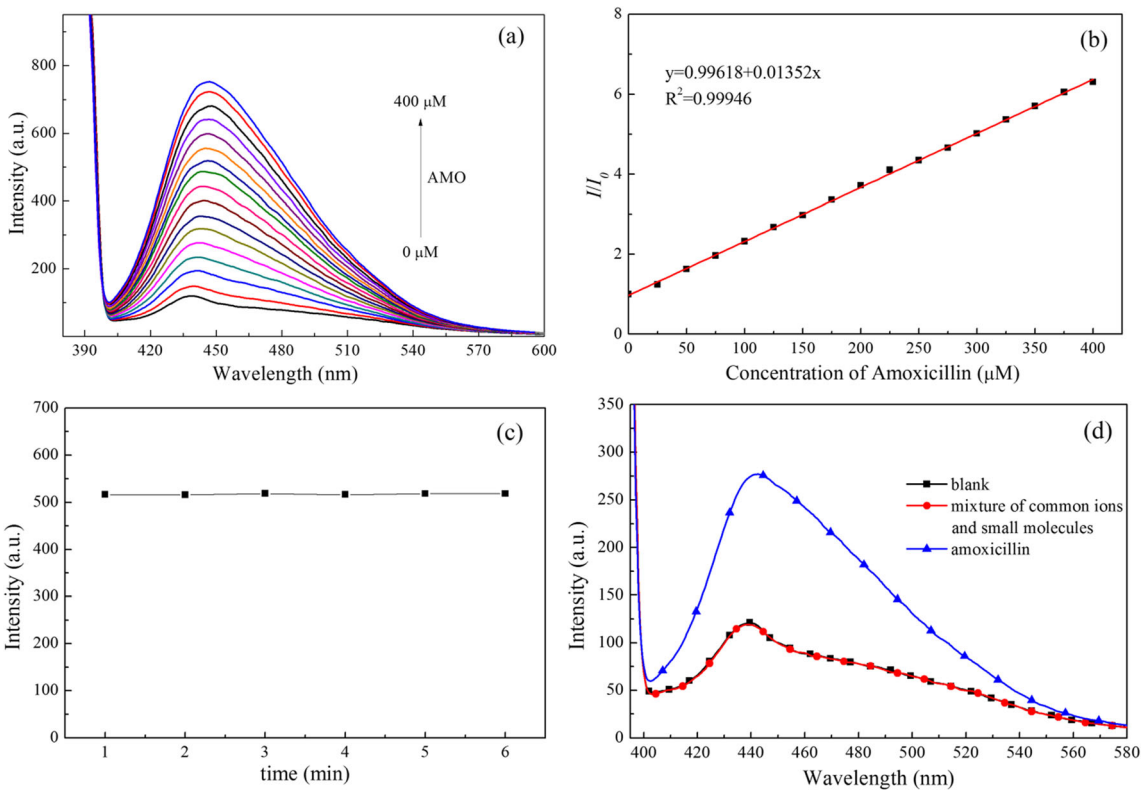

Fig. 6 **a** PL spectra of CQDs dispersion in the presence of different concentrations of AMO from 0 to 400 μM. CQDs, 5 μg·mL^{-1}, **b** the linear plot of I/I_0 versus AMO concentration in the range from 0 to 400 μM, **c** Time-dependent PL response of CQDs in PBS (pH 6.8). CQDs, 5 μg·mL^{-1}, **d** the PL intensity of the as-prepared CQDs (5 μg·mL^{-1}) in the presence of various common ions and small molecules (250 μM for each). Data are presented as average from three independent measurements ($N = 3$)

Conclusion

In this work, CQDs were synthesized using beet through a one-step hydrothermal process without any other chemical agents and further functionalization, a fast, green, low cost and convenient method to prepare fluorescent CQDs in large scale. It could be concluded that the as-prepared CQDs exhibit excellent water solubility and strong PL. The PL intensity I/I_0 showed a linear response with the concentration of AMO in a broad range 0-400 μM with a lower limit of detection of 0.475 μM. With all the virtues of CQDs prepared in the present work, a fast response, stable, highly sensitive and selective detecting method has established for the quantitative measurement of trace amount of AMO.

Acknowledgements This work was supported by grant No. 1508RJZA078 of the Natural Science Foundation of Gansu, the hongliu young teacher cultivate project of Lanzhou University of Technology (Q201211) and the Doctoral research start-funded projects of Lanzhou University of Technology.

Compliance with Ethical Standards

Conflicts of Interest There are no conflicts to declare.

References

1. De Baere S, De Backer P (2007) Quantitative determination of amoxicillin in animal feed using liquid chromatography with tandem mass spectrometric detection. Anal Chim Acta 586:319–325. https://doi.org/10.1016/j.aca.2006.10.036
2. Bergamini MF, Teixeira MFS, Dockal ER et al (2006) Evaluation of different voltammetric techniques in the determination of amoxicillin using a carbon paste electrode modified with [N, N'-ethylenebis(salicylideneaminato)] oxovanadium(IV). J Electrochem Soc 153:E94–E98. https://doi.org/10.1149/1.2184035
3. Shah K, Hassan E, Ahmed F et al (2017) Novel fluorene-based supramolecular sensor for selective detection of amoxicillin in water and blood. Ecotoxicol Environ Saf 141:25–29. https://doi.org/10.1016/j.ecoenv.2017.03.003
4. Cohen ML (1992) Epidemiology of Drug Resistance: Implications for a Post-Antimicrobial Era. Science 257(80):1050–1055. https://doi.org/10.1126/science.257.5073.1050
5. Gonzales R, Bartlett JG, Besser RE et al (2001) Principles of appropriate antibiotic use for treatment of acute respiratory tract infections in adults: background, specific aims, and methods. Ann Emerg Med 37:690–697. https://doi.org/10.1067/S0196-0644(01)70087-X
6. Hoizey G, Lamiable D, Frances C et al (2002) Simultaneous determination of amoxicillin and clavulanic acid in human plasma by HPLC with UV detection. J Pharm Biomed Anal 30:661–666. https://doi.org/10.1016/S0731-7085(02)00289-3
7. Fuwei W, Jinghua Y, Ping D, Shenguang G (2010) Molecular imprinting-Chemiluminescence sensor for the determination of amoxicillin. Anal Lett 43:1033–1045. https://doi.org/10.1080/00032710903491104
8. Straub RF, Voyksner RD (1993) Determination of penicillin G, ampicillin, amoxicillin, cloxacillin and cephapirin by high-performance liquid chromatography-electrospray mass spectrometry. J Chromatogr A 647:167–181. https://doi.org/10.1016/0021-9673(93)83336-Q
9. Abdulghani AJ, Jasim HH, Hassan AS (2012) Determination of β-lactam antibiotics in pharmaceutical preparations by Uv-visible spectrophotometry atomic absorption and high performance liquid chromatography. Pakistan J Chem 2:150–160. https://doi.org/10.15228/2012.v02.i03.p08
10. Ojani R, Raoof J-B, Zamani S (2012) A novel voltammetric sensor for amoxicillin based on nickel-curcumin complex modified carbon paste electrode. Bioelectrochemistry 85:44–49. https://doi.org/10.1016/j.bioelechem.2011.11.010
11. Xu X, Ray R, Gu Y et al (2004) Electrophoretic analysis and purification of fluorescent single-walled carbon nanotube fragments. J Am Chem Soc 126:12736–12737. https://doi.org/10.1021/ja040082h
12. Hutton GAM, Martindale BCM, Reisner E (2017) Carbon dots as photosensitisers for solar-driven catalysis. Chem Soc Rev 46:6111–6123. https://doi.org/10.1039/C7CS00235A
13. Wang F, Chen P, Feng Y et al (2017) Facile synthesis of N-doped carbon dots/g-C_3N_4 photocatalyst with enhanced visible-light photocatalytic activity for the degradation of indomethacin. Appl Catal B Environ 207:103–113. https://doi.org/10.1016/j.apcatb.2017.02.024
14. Zhang J, Yu SH (2016) Carbon dots: large-scale synthesis, sensing and bioimaging. Mater Today 19:382–393. https://doi.org/10.1016/j.mattod.2015.11.008
15. Shangguan J, Huang J, He D et al (2017) Highly Fe^{3+}-selective fluorescent Nanoprobe based on Ultrabright N/P Codoped carbon dots and its application in biological samples. Anal Chem 89:7477–7484. https://doi.org/10.1021/acs.analchem.7b01053
16. Hou J, Dong J, Zhu H et al (2015) A simple and sensitive fluorescent sensor for methyl parathion based on l-tyrosine methyl ester functionalized carbon dots. Biosens Bioelectron 68:20–26. https://doi.org/10.1016/j.bios.2014.12.037
17. Tan J, Zou R, Zhang J et al (2016) Large-scale synthesis of N-doped carbon quantum dots and their phosphorescence properties in a polyurethane matrix. Nano 8:4742–4747. https://doi.org/10.1039/C5NR08516K
18. Zhang C, Cui Y, Song L et al (2016) Microwave assisted one-pot synthesis of graphene quantum dots as highly sensitive fluorescent probes for detection of iron ions and pH value. Talanta 150:54–60. https://doi.org/10.1016/j.talanta.2015.12.015
19. Sharma S, Mehta SK, Kansal SK (2017) Highly fluorescent silver oxide/C-dots nanocomposite as selective and sensitive probe for highly efficient detection of Fe(III) ions. Sensors Actuators B Chem 243:1148–1156. https://doi.org/10.1016/j.snb.2016.12.100
20. Atchudan R, Edison TNJI, Chakradhar D et al (2017) Facile green synthesis of nitrogen-doped carbon dots using Chionanthus retusus fruit extract and investigation of their suitability for metal ion sensing and biological applications. Sensors Actuators B Chem 246:497–509. https://doi.org/10.1016/j.snb.2017.02.119
21. Wang J, Qiu F, Wu H et al (2017) Fabrication of fluorescent carbon dots-linked isophorone diisocyanate and β-cyclodextrin for detection of chromium ions. Spectrochim Acta Part A Mol Biomol Spectrosc 179:163–170. https://doi.org/10.1016/j.saa.2017.02.031
22. Tabaraki R, Abdi O, Yousefipour S (2017) Green and selective fluorescent sensor for detection of Sn (IV) and Mo (VI) based on boron and nitrogen-co-doped carbon dots. J Fluoresc 27:651–657. https://doi.org/10.1007/s10895-016-1994-x
23. Liu H, He Z, Jiang LP, Zhu JJ (2015) Microwave-assisted synthesis of wavelength-tunable Photoluminescent carbon Nanodots and their potential applications. ACS Appl Mater Interfaces 7:4913–4920. https://doi.org/10.1021/am508994w
24. Guo Y, Wang Z, Shao H, Jiang X (2013) Hydrothermal synthesis of highly fluorescent carbon nanoparticles from sodium citrate and

their use for the detection of mercury ions. Carbon N Y 52:583–589. https://doi.org/10.1016/j.carbon.2012.10.028
25. Gonçalves HMR, Duarte AJ, Esteves da Silva JCG (2010) Optical fiber sensor for hg(II) based on carbon dots. Biosens Bioelectron 26:1302–1306. https://doi.org/10.1016/j.bios.2010.07.018
26. Yang K, Wang S, Wang Y et al (2017) Dual-channel probe of carbon dots cooperating with gold nanoclusters employed for assaying multiple targets. Biosens Bioelectron 91:566–573. https://doi.org/10.1016/j.bios.2017.01.014
27. Simões EFC, Esteves da Silva JCG, Leitão JMM (2015) Peroxynitrite and nitric oxide fluorescence sensing by ethylenediamine doped carbon dots. Sensors Actuators B Chem 220:1043–1049. https://doi.org/10.1016/j.snb.2015.06.072
28. Luo M, Hua Y, Liang Y et al (2017) Synthesis of novel β-cyclodextrin functionalized S, N codoped carbon dots for selective detection of testosterone. Biosens Bioelectron 98:195–201. https://doi.org/10.1016/j.bios.2017.06.056
29. Yang W, Ni J, Luo F et al (2017) Cationic carbon dots for modification-free detection of Hyaluronidase via an electrostatic-controlled Ratiometric fluorescence assay. Anal Chem 89:8384–8390. https://doi.org/10.1021/acs.analchem.7b01705
30. Devi P, Kaur G, Thakur A et al (2017) Waste derivitized blue luminescent carbon quantum dots for selenite sensing in water. Talanta 170:49–55. https://doi.org/10.1016/j.talanta.2017.03.069
31. Li Z, Zhang J, Li Y et al (2018) Carbon dots based photoelectrochemical sensors for ultrasensitive detection of glutathione and its applications in probing of myocardial infarction. Biosens Bioelectron 99:251–258. https://doi.org/10.1016/j.bios.2017.07.065
32. Hou J, Li H, Wang L et al (2016) Rapid microwave-assisted synthesis of molecularly imprinted polymers on carbon quantum dots for fluorescent sensing of tetracycline in milk. Talanta 146:34–40. https://doi.org/10.1016/j.talanta.2015.08.024
33. Li H, Kang Z, Liu Y, Lee ST (2012) Carbon nanodots: synthesis, properties and applications. J Mater Chem 22:24230. https://doi.org/10.1039/c2jm34690g
34. Lim SY, Shen W, Gao Z (2015) Carbon quantum dots and their applications. Chem Soc Rev 44:362–381. https://doi.org/10.1039/C4CS00269E
35. Han T, Yan T, Li Y et al (2015) Eco-friendly synthesis of electrochemiluminescent nitrogen-doped carbon quantum dots from diethylene triamine pentacetate and their application for protein detection. Carbon N Y 91:144–152. https://doi.org/10.1016/j.carbon.2015.04.053
36. Wang K, Guan F, Li H et al (2015) One-step synthesis of carbon nanodots for sensitive detection of cephalexin. RSC Adv 5:20511–20515. https://doi.org/10.1039/C4RA15433A
37. Li X, Zhang S, S a K et al (2015) Engineering surface states of carbon dots to achieve controllable luminescence for solid-luminescent composites and sensitive Be^{2+} detection. Sci Rep 4:4976. https://doi.org/10.1038/srep04976
38. Wang K, Wang X, Li M et al (2016) Chemiluminescence of O-doped carbon Nanodots prepared in acidic and alkaline conditions. J Biomater Tissue Eng 6:35–41. https://doi.org/10.1166/jbt.2016.1411
39. Yang M, Li H, Liu J et al (2014) Convenient and sensitive detection of norfloxacin with fluorescent carbon dots. J Mater Chem B 2:7964–7970. https://doi.org/10.1039/C4TB01385A
40. Niu J, Gao H (2014) Synthesis and drug detection performance of nitrogen-doped carbon dots. J Lumin 149:159–162. https://doi.org/10.1016/j.jlumin.2014.01.026